Journal Pre-proof

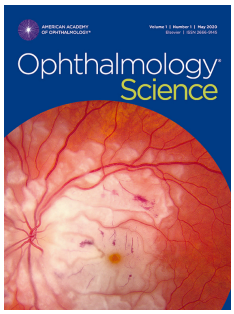

Fundus Stretch Index: a centile-based retinal measure of myopia

Fabian Yii, PhD

PII: S2666-9145(26)00100-4

DOI: https://doi.org/10.1016/j.xops.2026.101162

Reference: XOPS 101162

To appear in: *Ophthalmology Science*

Received Date: 3 December 2025

Revised Date: 27 February 2026

Accepted Date: 10 March 2026

Please cite this article as: Yii F., Fundus Stretch Index: a centile-based retinal measure of myopia, *Ophthalmology Science* (2026), doi: https://doi.org/10.1016/j.xops.2026.101162.

Fundus Stretch Index: a centile-based retinal measure of myopia

Fabian Yii, *PhD*[1,2,3,4]

1. Robert O Curle Ophthalmology Suite, Institute for Regeneration and Repair, The University of Edinburgh, UK
2. Centre for Clinical Brain Sciences, Institute for Neuroscience and Cardiovascular Research, The University of Edinburgh, UK
3. Centre for Population Health Sciences, Usher Institute, The University of Edinburgh, Edinburgh, UK
4. Department of Twin Research and Genetic Epidemiology, King's College London, London, UK

Correspondence
Fabian Yii
49 Little France Crescent,
Edinburgh EH16 4SB, UK
fabian.yii@ed.ac.uk

Financial Support: F Yii acknowledges funding support from the UKRI Medical Research Council in the form of a Transition Fellowship (MR/W006804/1). The funder had no role in the design or conduct of this study, nor the decision to submit this manuscript for publication.

Conflict of Interest: No conflicting relationship exists for the author.

Running Head: FunSI as an explainable retinal measure of myopia

Data Availability: This research was conducted using data from the UK Biobank under project ID 90655. Researchers interested in using the data can apply for access at ukbiobank.ac.uk/enable-your-research/apply-for-access. The source code is freely available at https://github.com/fyii200/FunSI.

Abbreviations and Acronyms: SER, spherical equivalent refraction; DL, deep learning; FunSI, fundus stretch index; FRO, fundus refraction offset; RD, retinal detachment; POAG, primary open-angle glaucoma; ICD-10, International Classification of Disease Version 10; OPCS-4, Office of Population Censuses and Surveys: Classification of Surgical Operations Version 4; IOP, intraocular pressure; CH, corneal hysteresis; HR, hazard ratio; CI, confidence intervals

Word Count: 3951

Keywords: Myopia, retina, fundus stretch index, fundus refraction offset, retinal detachment, glaucoma

This article contains additional online-only material. The following should appear online-only: Tables S1, S2, S3, S4, S5, S6, S7 and S8.

Abstract

Objective: To propose and evaluate the risk-stratification potential of Fundus Stretch Index (FunSI), a centile-based retinal metric that quantifies the geometric deviation of the fundus from what is expected for a given spherical equivalent refraction (SER).

Design: Population-based cohort study.

Participants: Phakic eyes of 25,222 adults (SER: 0D to -12D) with adequate-quality fundus photographs at baseline (2009-2010), individually linked to routinely collected health records until 2022.

Methods: Quantile regression was used to estimate the 5th to 95th centiles of 10 dimensionless fundus imaging features (e.g. arterial/venous tortuosity, disc tilt), conditioning on SER. FunSI was computed as the sum of an eye's SER-specific centile position across all imaging features, normalised to 0-1, such that an eye consistently ranked in the *worst* centile (5th or 95th, depending on the direction of change as myopia increased) for its SER would have a value of 1. Cox regression was used to test the association between baseline FunSI and the risk of: rhegmatogenous retinal detachment (RD), adjusting for baseline SER, age, sex, ethnicity, Townsend deprivation index, diabetes, hypertension and ocular trauma; and primary open-angle glaucoma (POAG), adjusting for the same baseline covariates (excluding ocular trauma) plus intraocular pressure and corneal hysteresis.

Main Outcomes and Measures: Rhegmatogenous RD and POAG onset.

Results: A total of 25,030 and 24,835 adults aged 40-69 years without any prior history of RD/breaks and glaucoma of any subtype were analysed, respectively. The event

rates (new cases per 10,000 person-years) were 4.9 for rhegmatogenous RD and 15.0 for POAG. Higher baseline FunSI was associated with an increased risk of developing rhegmatogenous RD (adjusted hazard ratio per 1 SD [0.09], 1.26; 95% confidence intervals, 1.08-1.48; *P*=.004) and POAG (1.11; 1.01-1.22; *P*=.03). The addition of FunSI led to a much clearer improvement in the concordance index for the rhegmatogenous RD model compared with the POAG model.

Conclusions: FunSI is an explainable approach to characterising myopia at the retinal level. Two individuals may share similar baseline risk factors such as SER, but an overall geometric difference in their fundi, as quantified by FunSI, may reveal a difference in their long-term risk of sight-threatening diseases.

Introduction

While increasing myopia is generally accompanied by retinal imaging changes suggestive of a progressively more stretched appearance (e.g. less tortuous and less densely branched vessels),[1-3] some fundi appear far more or far less stretched than would be expected for their degree of myopia. Such discrepancies are partly attributable to the limitation of conventional measures of myopia, which focus on the axial dimension of the eye (visual axis), to describe what is fundamentally a three-dimensional process: ocular growth.[4] Two eyes may have identical spherical equivalent refraction (SER) yet differ markedly in their posterior segment shape, giving rise to different off-axis retinal morphology.[4]

An interesting question arising from this brief discussion is whether quantitative information from across an individual's fundus can be incorporated into SER to develop a more individualised, "retinal measure" of myopia.[1] One approach is to use deep learning (DL) to predict SER directly from a colour fundus photograph. The premise is that, assuming a good bias-variance trade-off, a DL model will have a more negative prediction error when applied to a fundus that appears more myopic than expected for the eye's SER.[5] This is analogous to how an "older appearing" fundus may indicate accelerated ageing (biological age > chronological age).[6, 7] One such DL-driven retinal measure of myopia is Fundus Refraction Offset (FRO), which has been shown to be predictive of future retinal detachment (RD), independently of baseline SER and relevant covariates.[5, 8] However, a downside of this approach is its reduced

explainability, as the measure is derived directly from raw fundus photographs instead of some readily interpretable imaging features (e.g. vessel tortuosity).

To improve clinical explainability, it may help to consider an alternative approach that has proved very useful in paediatrics: growth chart.[9] At its most basic level, a growth chart displays various centiles of a physical parameter, such as height, as a function of age. A child positioned on the 98th centile, for example, is unusually tall for his/her age (98% of children of the same age are shorter). By substituting height with a fundus imaging feature and age with SER, one could similarly create a fundus centile chart to determine how typical, or atypical, an eye is for its SER. With several such centile charts, each based on a different imaging feature, it may be possible to get an overall picture of how quantitatively different a fundus is relative to other eyes with similar SER. Here, the author introduced an explainable retinal measure of myopia based on this concept, Fundus Stretch Index (FunSI), and investigated its longitudinal association with rhegmatogenous RD and primary open-angle glaucoma (POAG), beyond the influence of baseline covariates including SER.[10]

Methods

Study participants

This study was reported in accordance with the Strengthening the Reporting of Observational Studies in Epidemiology (STROBE) guidelines.[11] The study participants were sourced from the UK Biobank Eye and Vision dataset, a large cohort of mid-life (40-69 years) adults recruited from various sites across England, Scotland and Wales. As the UK Biobank has Research Tissue Bank approval from the Northwest Multi-Center Research Ethics Committee (06/MRE08/65), no separate ethical clearance was required. All participants provided informed consent, and the study adhered to the Declaration of Helsinki.

The reader is referred to previous publications for a detailed description of this cohort.[12, 13] Briefly, between 2009 and 2010, 68,508 individuals participated in a range of baseline physical and ophthalmic assessments, including 45-degree macula-centred colour fundus photography (Topcon 3D OCT-1000 Mark II) and autorefraction (Tomey RC-5000). In addition to in-person follow-up visits every few years, each individual was linked to the national death registries (2006-2022 for all 3 UK constituent countries) and routinely collected health-related datasets from the UK publicly funded healthcare system, the National Health Services (NHS). These included primary care (1938–2016 for England, 1939–2017 for Scotland and 1948–2017 for Wales) and hospital admission/procedural records (1981–2022 for Scotland, 1991–2022 for Wales and 1997–2022 for England).

Eligibility criteria

Figure 1 summarises the flow of participants through each stage of the selection process. Initially, 51,086 individuals with at least one eye passing a previously described and validated image quality assessment were included.[1, 14] Eyes with SER > 0D were subsequently excluded, and those in which one or more imaging features failed computation due to poor image segmentation were further removed. Likewise, eyes lying outside the top and bottom 0.1% of the distribution of any imaging features were excluded, as these outliers were caused by poor image segmentation upon visual inspection.

As very few eyes (n=209) had extreme myopia above 12D, centile estimates (described in the next subsection) could not be obtained precisely beyond this level of myopia; these eyes were therefore removed. To rule out the influence of pseudophakia, the author also excluded individuals with a self-reported history of cataract/refractive surgery (UK Biobank data-fields 5324 and 5325) or those with a 3-digit procedural code related to lens extraction based on the Office of Population Censuses and Surveys: Classification of Surgical Operations Version 4 (OPCS-4), namely C71, C72 and C74, on or prior to the baseline visit. Following this, 40,258 eyes of 25,222 individuals were finally included.

Centile-based Fundus Stretch Index

A range of fundus imaging features were computed using automated pipelines described in previous work.[1, 15] To mitigate the optical influence of ocular magnification,

and to avoid assuming any specific camera design (e.g. telecentricity) or resolution (mm per pixel),[16] only dimensionless imaging features were considered when calculating FunSI. These features (n=10) are summarised in Table 1 and further detailed elsewhere.[1, 15]

Quantile regression with non-crossing constraints[17, 18] was used to estimate the 5th to 95th centiles (in 5-centile increments) of each imaging feature, conditioning on SER and using data from one randomly selected eye when both eyes of an individual were available. As shown in Figure 2, this resulted in 10 centile charts (one per imaging feature), each containing 19 centile curves. A key advantage of quantile regression is that it makes no assumptions about the conditional distribution of the dependent variable, in contrast to the less flexible semi-parametric Lambda-Mu-Sigma method.

The FunSI for each of the 40,258 eligible eyes was calculated by summing its SER-specific centile position across the 10 centile charts per Equation 1, followed by min-max normalisation of this sum to a range of 0-1 per Equation 2. A FunSI of 0.5 would therefore suggest an “average-looking” fundus given the eye’s SER, while a fundus consistently ranked in the worst centile across all imaging features would have a FunSI of 1. For each imaging feature, the worst centile was either the 5th or the 95th centile, depending on the direction of change of that feature as myopia increased. For example, the worst centile for arterial tortuosity was the 5th centile because tortuosity generally decreased with myopia, and vice versa for arterial concavity.[1]

[1] $Cent_{sum} = Cent_{arterial\ concavity} + Cent_{venous\ concavity} + Cent_{DFD:DML} + Cent_{disc\ tilt} + (1\text{-}Cent_{arterial\ FD}) + (1\text{-}Cent_{venous\ FD}) + (1\text{-}Cen_{AVR}) + (1\text{-}Cent_{arterial\ tortuosity}) + (1\text{-}Cent_{venous\ tortuosity}) + (1\text{-}Cent_{absolute\ disc\ torsion})$

[2] $FunSI = (Cent_{sum} - 0.5) / 9$

Where *Cent* represents the decimal centile position (e.g. 0.5 for the 50th centile), determined by identifying the centile curve closest to the observed value of a given imaging feature (capped at the 5th and 95th centiles); *DFD:DML* represents the ratio of disc-fovea distance to disc major axis length; *FD* represents fractal dimension; and *AVR* represents arteriovenous ratio. Because the 5th centile (0.05) represented the worst centile for arterial/venous FD, AVR, arterial/venous tortuosity and absolute disc torsion, subtracting *Cent* corresponding to these imaging features from 1 ensured that a FunSI closer to 1 reflected a more structurally myopic retina. Figure 3 shows some examples of eyes with similar SER but different FunSI.

Events of interest

Using a combination of sources including NHS records mentioned earlier and touch-screen questionnaires administered during each assessment visit (self-reported history), the UK Biobank team has made the first-occurrence date of RD/breaks and glaucoma available as data-fields 131178 and 131186, respectively.[19] However, these were mapped to the first three characters of the International Classification of Disease Version 10 (ICD-10) codes, encompassing various subtypes of RD/breaks (H33) and glaucoma (H40). The source hospital records of individuals with RD/breaks (H33) based on data-field 131178 were accessed to ascertain cases of rhegmatogenous RD (H33.0), given that patients with rhegmatogenous RD would almost certainly require hospital

treatment. For POAG, an elimination approach was applied by defining it as the presence of glaucoma (H40) according to data-field 131186 but without: (1) any ICD-10 codes related to primary angle-closure glaucoma (H40.2), secondary glaucoma (H40.3 to H40.6), other glaucoma (H40.8) and glaucoma in other diseases (H42.0 and H42.8); as well as (2) any OPCS-4 codes related to angle-closure glaucoma, namely iridosclerotomy (C62.1) and iridotomy (C62.2 and C62.3).

Populations at risk and observation period

For the analyses described below, the population at risk for rhegmatogenous RD comprised individuals with no prior history of RD/breaks of any subtype (e.g. rhegmatogenous, tractional, serous), by excluding those with an ICD-10 code H33 (data-field 131178) recorded on or before the baseline visit. Likewise, the population at risk for POAG comprised individuals without glaucoma of any subtype (including angle-closure glaucoma) recorded on or before the baseline visit (ICD-10 code H40; data-field 131186). The observation period (follow-up time) spanned from an individual's baseline visit (2009-2010) to the right-censoring date, defined as the earliest of: last day of 2022, date of death or date of loss to follow-up due to emigration or withdrawal of consent for future data linkage. For rhegmatogenous RD analyses, the observation period was additionally right-censored at cataract surgery, given the potential confounding effect of cataract surgery during follow-up.[20] To account for competing risks, the observation period was also right censored at the first occurrence of non-rhegmatogenous RD (for rhegmatogenous RD analyses) or glaucoma unrelated to POAG (for POAG analyses). No individual had zero follow-up time.

Statistical (survival) analysis

All statistical analyses were performed at the individual level because laterality information was not available for the events, averaging continuous data across eyes when both eyes of an individual were eligible (unless otherwise stated).

Kaplan-Meier plots were used to visualise the cumulative incidence ([1-survival probability] X 100) of each event over time, stratified by baseline FunSI (categorised into 4 quantiles for visualisation purposes). Multivariable Cox regression models were then fitted to test the association between baseline FunSI (continuous) and time to each event, defined as the time elapsed from the baseline visit to the first-occurrence date or the right-censoring date (whichever came first). Note that FunSI was standardised to zero mean and unit variance in all models to place the estimated hazard ratio (HR) on a less steep and more interpretable scale, such that an HR of x represented an x-fold change in hazard rate for every 1 standard deviation (SD) change in FunSI, rather than per 1-unit change in the index (which would unrealistically reflect a change across the full 0-1 theoretical range of FunSI). The models initially assumed a linear relationship and were then extended to include non-linear FunSI terms: a second-degree polynomial ($FunSI + FunSI^2$), followed by a third-degree polynomial ($FunSI + FunSI^2 + FunSI^3$).

Covariate adjustment

Baseline covariates selected a priori and adjusted for in each model included basic/common demographic and clinical information: age (continuous), sex (binary), SER (continuous: spherical power + cylindrical power/2), Townsend deprivation index

(continuous: positive values indicated higher deprivation), ethnicity (binary: White vs non-white), diabetes (Boolean) and hypertension (Boolean). History of ocular trauma (Boolean) was additionally included in the rhegmatogenous RD model, while intraocular pressure (IOP) and corneal hysteresis (CH),[21] both of which were continuous variables measured with the Reichert Ocular Response Analyser, were additionally included in the POAG model. Unreasonable IOP (0 or >45 mmHg)[22] and CH (0 or >15 mmHg)[23-25] values were removed (treated as missing), as these were most likely caused by measurement error. The reader is referred to Yii et al.[8] for further information about each covariate.

Leave-one-feature-out, sensitivity and subgroup analyses

To assess the relative influence of each imaging feature on the Cox regression results, FunSI was recomputed using a leave-one-feature-out approach (one feature omitted at a time). Additionally, sensitivity analyses were conducted by: (1) excluding self-reported cases and cases not identified through hospital records (this analysis was not applicable to rhegmatogenous RD because, by definition, all cases had a hospital record); (2) excluding individuals with cylindrical power >2D to rule out the potential influence of refractive myopia (e.g. due to keratoconus); (3) excluding cases occurring within 1 year of baseline to rule out any inadvertent inclusion of prevalent cases resulting from a potential time lag between disease onset and the availability of records; (4) selecting FunSI and covariate data from the more myopic eye when both eyes were eligible; and (5) lowering the imaging feature outlier threshold (as described under the eligibility criteria) from 0.1% to 0.01% (thus excluding fewer eyes). Finally, in a subgroup of

individuals not previously used to train the FRO DL model,[5] baseline FRO was included as an additional continuous covariate (subgroup analysis).

The variance inflation factor was <1.2 in all fitted models, indicating no evidence of multicollinearity. A complete-case approach was used to handle missing data when the data could be assumed to be missing completely at random (MCAR), based on Little's test.[26, 27] Otherwise, multiple (n=10) imputation using the predictive mean matching method[28] was performed. The concordance index (C-index) was used to summarise the discriminative ability of the fitted models, with higher values indicating better discrimination.[29] All analyses were performed in R V.4.5.1 (R Core Team, Vienna, Austria), using the *quantregGrowth* and *survival* packages for centile curve estimation and survival analyses, respectively. The source code is openly available at https://github.com/fyii200/FunSI. Hypothesis testing was 2-tailed, with $P<.05$ considered sufficient evidence to reject the null hypotheses.

Results

Baseline characteristics and cumulative incidence

Table 2 summarises the baseline characteristics of the populations at risk for rhegmatogenous RD and POAG. For rhegmatogenous RD, 25,030 (99.9%) of 25,067 at-risk individuals had complete data; 37 individuals with missing Townsend deprivation index were excluded from all analyses, as the MCAR assumption was met (χ^2=6.4; *P*=.79). For POAG, 23,600 (95.0%) of 24,835 at-risk individuals had complete data; missing values for CH (n=1191), IOP (n=750) and Townsend deprivation index (n=37) were imputed, as the MCAR assumption was violated (χ^2=584.4; *P*<.001).

The mean (SD) observation period was 12.0 (2.1) for rhegmatogenous RD (301,348 person-years) and 12.3 (1.6) years for POAG (306,179 person-years). A total of 148 individuals had incident rhegmatogenous RD during the observation period, yielding an event rate of 4.9 cases per 10,000 person-years. The number of incident POAG cases was 460, corresponding to an event rate of 15.0 cases per 10,000 person-years. Of these POAG cases, 23 were self-reported and 437 were identified through other sources, including 319 through hospital records.

The cumulative incidence of each event over time, stratified by baseline FunSI, is shown in Figure 4. Compared with individuals in the lowest FunSI quantile, those in the highest FunSI quantile had twice as high cumulative incidence of rhegmatogenous RD over 12 years (0.8% [95% CI: 0.6% to 1.1%] vs 0.4% [0.3% to 0.6%]). Similarly, the 12-

year cumulative incidence of POAG was more than twice as high in the highest FunSI quantile (2.5% [2.1% to 2.9%]) as that observed in the lowest FunSI quantile (1.2% [0.9% to 1.4%]).

Multivariable Cox regression

As shown in Table 3, higher baseline FunSI was associated with an increased risk of developing rhegmatogenous RD (adjusted HR per 1 SD [0.09], 1.26; 95% CI, 1.08 to 1.48; *P*=.004) and POAG (1.11; 1.01 to 1.22; *P*=.03), even after adjusting for baseline covariates including SER (univariable associations are presented in Table S1). The C-index for the rhegmatogenous RD model without FunSI was 0.689, increasing by 0.017 to 0.706 when FunSI was added. In contrast, the addition of FunSI to the POAG model only led to a very modest increase in the C-index (+0.003, from 0.804 to 0.807).

Addition of non-linear terms

None of the non-linear FunSI terms were associated with the risk of rhegmatogenous RD, whether modelled as a second-degree polynomial (*P*=.39 for $FunSI^2$) or a third-degree polynomial (*P*=.55 for $FunSI^2$ and *P*=.19 for $FunSI^3$). There was some weak indication of a quadratic relationship between FunSI and POAG risk: in the second-degree polynomial model, the $FunSI^2$ term was associated with disease risk (HR, 0.90; 95% CI, 0.82 to 1.00; *P*=.046), but its inclusion did not improve the C-index (0.806, similar to the original linear model).

Leave-one-feature-out, sensitivity and subgroup analyses

Findings from the leave-one-feature-out analysis are presented in Table S2. Baseline FunSI remained associated (*P*<.05) with rhegmatogenous RD risk regardless of which imaging feature was removed, with estimated HRs ranging from 1.19 to 1.30. For POAG, however, baseline FunSI was no longer associated with disease risk after removing *DFD:DML*, arterial/venous FD or AVR, suggesting that these features had a disproportionate influence on FunSI's association with POAG risk.

The overall conclusions—that higher baseline FunSI was associated with an increased risk of rhegmatogenous RD and POAG—remained unchanged after repeating the multivariable Cox regression across all 5 sensitivity analyses: (1) exclusion of self-reported and non-hospital cases (Table S3); (2) exclusion of individuals with cylindrical power >2D (Table S4); (3) exclusion of cases occurring within 1 year of baseline (Table S5); (4) analysis of data from the more myopic eye (Table S6); and (5) lowering the imaging feature outlier threshold to 0.01% (Table S7).

In the subgroup analysis, 104 of 15,954 eligible individuals had incident rhegmatogenous RD, and 335 of 15,754 had incident POAG. As shown in Table S8, baseline FRO (adjusted HR per 1 SD [0.87D], 0.77; 95% CI, 0.65 to 0.90; *P*=.002) and FunSI (1.29; 1.07 to 1.57; *P*=.009) were both independently associated with the risk of developing rhegmatogenous RD. The C-index was 0.679 for the rhegmatogenous RD model without FRO and FunSI, increasing by 0.021 to 0.700 after adding FRO, and further increased by 0.018 to 0.718 with the inclusion of FunSI—an overall improvement

of almost 0.04. For POAG, there was insufficient evidence to suggest that FRO (0.91; 0.82 to 1.00; *P*=.053) and FunSI (1.09; 0.98 to 1.22; *P*=.10) were independently associated with disease risk, although some trends were observed. Accordingly, the changes in the C-index attributable to FRO (+0.001) and FunSI (+0.001) were practically absent, with a negligible overall improvement of 0.002 from 0.796 to 0.798.

Discussion

The present study introduced FunSI, a retinal measure of myopia that summarises an eye's SER-specific centile position across a range of explainable fundus imaging features (Table 1), where a higher value suggests a more stretched fundus relative to the eye's SER. As demonstrated in the primary analysis, individuals with similar SER and other baseline risk factors may nonetheless exhibit geometric differences in their fundi, as summarised by FunSI, which may translate into differences in the risk of developing rhegmatogenous RD (or, to a lesser extent, POAG) over the subsequent 12 years.

In the subgroup analysis, both baseline FunSI and FRO[5, 8] were found to be associated with the risk of developing rhegmatogenous RD, independently of one another. Indeed, a post-hoc linear regression of FRO on FunSI showed that, while a higher FunSI was associated (*P*=.01) with a more negative FRO (more myopic-looking fundus as inferred by DL), the strength of association was weak, where a 1 SD increase in FunSI was only associated with -0.02D (95% CI, -0.03D to -0.003D) change in FRO. Both measures are thus complementary, as they appear to capture different retinal information pertinent to myopia. However, when considering POAG as the event in the subgroup analysis, both FRO and FunSI were not associated with the disease, although some trends were observed. Compared with rhegmatogenous RD (Table 3), the association between FunSI and POAG in the primary analysis also appeared weaker (HR: 1.26 vs 1.11) and more uncertain, with the lower bound of 95% CI closer to the null. Additionally, the

improvement in the C-index attributable to FunSI was substantially smaller for the POAG model than for the rhegmatogenous RD model, in both the primary and subgroup analyses. Taken together, the evidence supporting FunSI (in its current form) as an independent risk marker for POAG is comparatively weaker.

A precursor to rhegmatogenous RD is the presence of vitreoretinal tractional forces acting on the neurosensory retina,[30, 31] which, as previously discussed,[8] may affect fundus appearance. Even when such tractional forces are not yet clinically evident, signs of strain imparted by an axially elongated, aspheric (more prolate or less oblate) posterior segment characteristic of a myopic eye may already be detectable, however subtly, at the pixel level across the fundus,[4] changes that could predispose the eye to rhegmatogenous RD.[32] Signs of myopic strain involving the optic nerve head (e.g. tilted and more obliquely orientated disc) and retinal vasculature (e.g. reduced FD) are also implicated in the increased susceptibility of myopic eyes to POAG, either mediated by a mechanical pathway or a perfusion-related pathway, or both.[33-36]

FunSI and, for that matter, FRO, differ from SER in being adjunctive measures of myopia that are more directly concerned with the structural characteristics of the retina. This emphasis may seem pedantic, but it closely aligns with recent high-profile consensus statements recommending that myopia be classified as a disease, first by the US National Academies of Science[37] and subsequently by the International Myopia Summit Workgroup.[38] The latter workgroup identified, as a “key strategy” for reducing the global burden of myopia, the need to define myopia not solely as a refractive error

but a disease with phenotypic features that influence long-term eye health outcomes.[38] This paradigm shift is an important step towards refining risk stratification in clinical practice,[38] as some patients with low myopia are at high risk of developing complications, far in excess of what is typical for their SER, whereas some highly myopic patients do not develop such complications. In practice, both FunSI and FRO provide the first proof of concept to advance this paradigm shift.

The male predilection to rhegmatogenous RD in this study (Table 3) is consistent with previous epidemiological findings.[39] Likewise, diabetes[40] and higher IOP[41] are two important risk factors for POAG, and mounting longitudinal evidence supports lower CH (reflecting reduced ability of ocular tissue to dissipate energy) as an independent risk factor for POAG onset,[42] including a recent UK Biobank study.[43]

Despite the use of a large-scale, population-based dataset, the fundus centile charts were derived from colour fundus photographs acquired with a Topcon camera. Although some degree of generalisability to other cameras may be expected, given that only dimensionless imaging features were considered, this requires external validation in future work. Likewise, further work is warranted to establish if the current version of FunSI is transferable across populations, given the predominance of a single ethnic group (White European) in the UK Biobank. As a proof of concept, this study lays the groundwork for other researchers to develop their own FunSI, with the potential for combining derived data in the future to create cross-population fundus centile charts. Another limitation is that It remains unclear whether FunSI is an independent measure

of myopia or a complex surrogate for axial length (AL) due to the absence of AL measurements in the UK Biobank. In addition to the need for external validation and adjustment for AL, future work could incorporate additional relevant imaging features, such as cup-to-disc ratio and degree of tessellation, to potentially improve the potential of FunSI for risk stratification. It would also be valuable for future longitudinal studies to investigate the association between FunSI and the risk of pathologic myopia or childhood myopia. Another interesting line of inquiry is to disentangle the potential relationships among FunSI, height, three-dimensional eye shape and eye volume.

In conclusion, FunSI is a promising, explainable retinal measure of myopia that may complement FRO in stratifying the risk of future rhegmatogenous RD—and, to a lesser extent, POAG—even among individuals with similar SER, age, sex and other baseline risk factors.

Figure legends

Figure 1. Participant flow diagram.

Figure 2. Fundus centile charts, one per imaging feature. Each chart consists of 19 centile curves, ranging from the 5th centile (very small value) to the 95th centile (very large value) in 5-centile increments. Centile curve corresponding to the 50th centile (median) is highlighted in red. DFD, disc-fovea distance.

Figure 3. Examples of colour fundus photographs with similar SER but different FunSI. SER, spherical equivalent refraction; FunSI, Fundus Stretch Index. Reproduced by kind permission of UK Biobank ©

Figure 4. Cumulative incidence (calculated as [1 - Kaplan-Meier survival probability] X 100) of rhegmatogenous retinal detachment and primary open-angle glaucoma over time, stratified by baseline FunSI (categorised into 4 quantiles for visualisation purposes). FunSI, Fundus Stretch Index.

Acknowledgement

F Yii acknowledges funding support from the UKRI Medical Research Council in the form of a Transition Fellowship (MR/W006804/1). Some materials from this study were presented at the UK Biobank Eye and Vision Consortium Annual Meeting in November 2025 (London, UK), Chinese Academy of Sciences in December 2025 (Hangzhou, China) and the 41st Asia-Pacific Academy of Ophthalmology Congress in February 2026 (Hong Kong, China SAR). The author would like to thank the audience for their insightful questions.

References

1. Yii F, Bernabeu MO, Dhillon B, et al. Retinal Changes from Hyperopia to Myopia: Not all Diopters are Created Equal. Invest Ophthalmol Vis Sci 2024;65(5):25.
2. Jonas JB, Spaide RF, Ostrin LA, et al. IMI-Nonpathological Human Ocular Tissue Changes With Axial Myopia. Invest Ophthalmol Vis Sci 2023;64(6):5.
3. Yii F, Gibbon S, MacGillivray T. Sectoral Changes in Neuroretinal Rim Pallor Across Refractive Error. Ophthalmol Sci 2025;5(3):100705.
4. Yii F, Strang NC, Gibbon S, MacGillivray TJ. Can fundus features tell us something about 3D eye shape? Ophthalmic Physiol Opt 2025.
5. Yii F, MacCormick IJC, Strang N, et al. Fundus Refraction Offset as an Individualized Myopia Biomarker. JAMA Ophthalmol 2025.
6. Zhu Z, Hu W, Chen R, et al. Retinal age gap as a predictive biomarker of stroke risk. BMC Med 2022;20(1):466.
7. Zhu Z, Chen Y, Wang W, et al. Association of Retinal Age Gap With Arterial Stiffness and Incident Cardiovascular Disease. Stroke 2022;53(11):3320-8.
8. Yii F, MacCormick IJC, Strang N, et al. Fundus Refraction Offset as a Personalized Biomarker for 12-Year Risk of Retinal Detachment. Invest Ophthalmol Vis Sci 2025;66(9):1.
9. Cole TJ. The development of growth references and growth charts. Ann Hum Biol 2012;39(5):382-94.
10. Haarman AEG, Enthoven CA, Tideman JWL, et al. The complications of myopia: A review and meta-analysis. Invest Ophthalmol Vis Sci 2020;61(4):49.
11. Elm Ev, Altman DG, Egger M, et al. Strengthening the reporting of observational studies in epidemiology (STROBE) statement: guidelines for reporting observational studies. BMJ 2007;335(7624):806.
12. Chua SYL, Thomas D, Allen N, et al. Cohort profile: design and methods in the eye and vision consortium of UK Biobank. BMJ Open 2019;9(2):e025077.
13. Sudlow C, Gallacher J, Allen N, et al. UK biobank: an open access resource for identifying the causes of a wide range of complex diseases of middle and old age. PLoS Med 2015;12(3):e1001779.
14. Fu H, Wang B, Shen J, et al. Evaluation of Retinal Image Quality Assessment Networks in Different Color-Spaces. In: Shen D, Liu T, Peters TM, et al., eds. Medical Image Computing and Computer Assisted Intervention – MICCAI 2019. Cham: Springer International Publishing, 2019.
15. Zhou Y, Wagner SK, Chia MA, et al. AutoMorph: Automated Retinal Vascular Morphology Quantification Via a Deep Learning Pipeline. Transl Vis Sci Technol 2022;11(7):12.
16. Yii F, Strang N, Moulson C, et al. The Optical Nature of Myopic Changes in Retinal Vessel Caliber. Ophthalmol Sci 2025;5(1):100631.
17. Muggeo VMR, Torretta F, Eilers PHC, et al. Multiple smoothing parameters selection in additive regression quantiles. Statistical Modelling 2020;21(5):428-48.
18. Wei Y, Pere A, Koenker R, He X. Quantile regression methods for reference growth charts. Stat Med 2006;25(8):1369-82.

19. UK Biobank. First Occurrence of Health Outcomes Defined by 3-character ICD10 code. Available from: https://biobank.ndph.ox.ac.uk/showcase/ukb/docs/first_occurrences_outcomes.pdf. 2019.
20. Lois N, Wong D. Pseudophakic retinal detachment. Surv Ophthalmol 2003;48(5):467-87.
21. Zimprich L, Diedrich J, Bleeker A, Schweitzer JA. Corneal Hysteresis as a Biomarker of Glaucoma: Current Insights. Clin Ophthalmol 2020;14:2255-64.
22. Chan MPY, Broadway DC, Khawaja AP, et al. Glaucoma and intraocular pressure in EPIC-Norfolk Eye Study: cross sectional study. BMJ 2017;358:j3889.
23. Narayanaswamy A, Su DH, Baskaran M, et al. Comparison of ocular response analyzer parameters in chinese subjects with primary angle-closure and primary open-angle glaucoma. Arch Ophthalmol 2011;129(4):429-34.
24. Kaushik S, Pandav SS, Banger A, et al. Relationship between corneal biomechanical properties, central corneal thickness, and intraocular pressure across the spectrum of glaucoma. Am J Ophthalmol 2012;153(5):840-9.e2.
25. Ayala M. Corneal hysteresis in normal subjects and in patients with primary open-angle glaucoma and pseudoexfoliation glaucoma. Ophthalmic Res 2011;46(4):187-91.
26. Tierney N, Cook D. Expanding Tidy Data Principles to Facilitate Missing Data Exploration, Visualization and Assessment of Imputations. Journal of Statistical Software 2023;105(7):1 - 31.
27. Roderick JAL. A Test of Missing Completely at Random for Multivariate Data with Missing Values. Journal of the American Statistical Association 1988;83(404):1198-202.
28. van Buuren S, Groothuis-Oudshoorn K. mice: Multivariate Imputation by Chained Equations in R. Journal of Statistical Software 2011;45(3):1 - 67.
29. Uno H, Cai T, Pencina MJ, et al. On the C-statistics for evaluating overall adequacy of risk prediction procedures with censored survival data. Stat Med 2011;30(10):1105-17.
30. Mitry D, Fleck BW, Wright AF, et al. Pathogenesis of rhegmatogenous retinal detachment: predisposing anatomy and cell biology. Retina 2010;30(10):1561-72.
31. Ghazi NG, Green WR. Pathology and pathogenesis of retinal detachment. Eye (Lond) 2002;16(4):411-21.
32. Lakawicz JM, Bottega WJ, Fine HF, Prenner JL. On the mechanics of myopia and its influence on retinal detachment. Biomech Model Mechanobiol 2020;19(2):603-20.
33. Wang YX, Panda-Jonas S, Jonas JB. Optic nerve head anatomy in myopia and glaucoma, including parapapillary zones alpha, beta, gamma and delta: Histology and clinical features. Prog Retin Eye Res 2021;83:100933.
34. Tan NYQ, Sng CCA, Ang M. Myopic optic disc changes and its role in glaucoma. Curr Opin Ophthalmol 2019;30(2):89-96.
35. Benavente-Perez A. Evidence of vascular involvement in myopia: a review. Front Med (Lausanne) 2023;10:1112996.
36. Chan KKW, Tang F, Tham CCY, et al. Retinal vasculature in glaucoma: a review. BMJ Open Ophthalmol 2017;1(1):e000032.
37. National Academies of Sciences, Engineering, and Medicine. Myopia: Causes, Prevention, and Treatment of an Increasingly Common Disease. Washington, DC: The National Academies Press, 2024; 374.

38. Eppenberger LS, Davis A, Resnikoff S, et al. Key strategies to reduce the global burden of myopia: consensus from the international myopia summit. Br J Ophthalmol 2025;109(5):535-42.
39. Mitry D, Charteris DG, Fleck BW, et al. The epidemiology of rhegmatogenous retinal detachment: geographical variation and clinical associations. Br J Ophthalmol 2010;94(6):678-84.
40. Zhou M, Wang W, Huang W, Zhang X. Diabetes mellitus as a risk factor for open-angle glaucoma: a systematic review and meta-analysis. PLoS One 2014;9(8):e102972.
41. Coleman AL, Miglior S. Risk factors for glaucoma onset and progression. Surv Ophthalmol 2008;53 Suppl1:S3-10.
42. Susanna CN, Diniz-Filho A, Daga FB, et al. A Prospective Longitudinal Study to Investigate Corneal Hysteresis as a Risk Factor for Predicting Development of Glaucoma. Am J Ophthalmol 2018;187:148-52.
43. Yun JS, Jung SH, Jung SM, et al. Corneal hysteresis as a biomarker in glaucoma development among patients with myopia: a prospective study based on the UK Biobank. Br J Ophthalmol 2025;109(9):997-1004.

Table 1. Description of each dimensionless (unitless) fundus imaging feature used to derive Fundus Stretch Index. The reader is kindly referred to Yii et al.[1] for further information about each imaging feature.

Fundus feature	Description
Arterial fractal dimension	Complexity of retinal arterioles. Larger values indicate increased complexity (more densely branched vasculature). Generally decreases with myopia.
Venous fractal dimension	Complexity of retinal venules. Larger values indicate increased complexity (more densely branched vasculature). Generally decreases with myopia.
Arteriovenous ratio	Ratio of central retinal arteriolar equivalent to central retinal venular equivalent. Larger values indicate *relative* arteriolar widening. Generally decreases with myopia.
Arterial tortuosity	Tortuosity of retinal arterioles. Larger values indicate more tortuous arterioles. Generally decreases with myopia.
Venous tortuosity	Tortuosity of retinal venules. Larger values indicate more tortuous venules. Generally decreases with myopia.
Arterial concavity	Parabolic course of the major temporal arterial arcade. Larger values indicate increased concavity (arterial arcade curves more inwardly towards the fovea). Generally increases with myopia.
Venous concavity	Parabolic course of the major temporal venous arcade. Larger values indicate increased concavity (venous arcade curves more inwardly towards the fovea). Generally increases with myopia.
Disc-fovea distance to disc major axis length ratio	Ratio of the Euclidian distance between the optic disc centroid and fovea (disc-fovea distance) to the *major axis length of the optic disc. A value of 3, for example, indicates that the disc-fovea distance is 3 times that of the major axis length of the optic disc. Generally increases with myopia.
Disc tilt	Ratio of the *major axis length of the optic disc to its *minor axis length. Larger values indicate a less circular, more oval optic disc appearance. Generally increases with myopia.
Absolute disc torsion (also known as disc orientation)	Absolute angle between horizontal axis of the image passing through the optic disc centroid and the *major axis of the optic disc (ranges from 0° to 90°). A vertically orientated optic disc will have a value of 90°. Generally decreases (less vertically orientated) with myopia.

**Based on the best-fitting ellipse*

Table 2. Baseline characteristics of participants included in the survival analyses. Continuous variables are presented as mean (standard deviation), and categorical variables as n (%).

Characteristics	**Rhegmatogenous RD** (n=25,030)	**Primary open-angle glaucoma** (n=24,835)
Age (year)	54.3 (8.1)	54.3 (8.1)
Female	13,513 (54.0)	13,430 (54.1)
White	22,742 (90.9)	22,572 (90.9)
SER (dioptre)	-2.12 (2.23)	-2.12 (2.23)
FunSI	0.50 (0.09)	0.50 (0.09)
Townsend deprivation index	-1.03 (2.95)	-1.04 (2.95)
Diabetes	1107 (4.4)	1080 (4.3)
Hypertension	5502 (22.0)	5440 (21.9)
Ocular trauma	124 (0.5)	/
Intraocular pressure (mmHg)	/	15.9 (3.5)
Corneal hysteresis (mmHg)	/	10.5 (1.7)

RD, *retinal detachment*; SER, *spherical equivalent refraction*; FunSI, *fundus stretch index*

Table 3. Adjusted association of baseline FunSI and covariates with each event (multivariable Cox regression).

Baseline variables	**Rhegmatogenous RD** (n=25,030)		**Primary open-angle glaucoma** (n=24,835)	
	Adjusted HR (95% CI)	*P*	Adjusted HR (95% CI)	*P*
SER, *per 1 dioptre*	0.81 (0.77 to 0.85)	<.001	0.93 (0.89 to 0.96)	<.001
FunSI, *per 1 SD (0.09)*	1.26 (1.08 to 1.48)	.004	1.11 (1.01 to 1.22)	.03
Age, *per 1 year*	1.00 (0.98 to 1.02)	.83	1.07 (1.05 to 1.08)	<.001
Male sex	1.89 (1.35 to 2.63)	<.001	1.14 (0.95 to 1.38)	.16
Townsend deprivation index, *per 1 unit*	0.97 (0.92 to 1.03)	.39	0.99 (0.96 to 1.02)	.55
White ethnicity	1.22 (0.63 to 2.35)	.56	0.66 (0.48 to 0.90)	.01
Diabetes	1.05 (0.48 to 2.30)	.89	1.58 (1.12 to 2.22)	.009
Hypertension	1.06 (0.71 to 1.57)	.78	1.12 (0.91 to 1.38)	.27
Ocular trauma	2.35 (0.58 to 9.50)	.23	/	/
IOP, *per 1 mmHg*	/	/	1.21 (1.19 to 1.23)	<.001
CH, *per 1 mmHg*	/	/	0.91 (0.86 to 0.96)	.001

RD, *retinal detachment*; HR, *hazard ratio*; CI, *confidence intervals*; SER, *spherical equivalent refraction*; FunSI, *fundus stretch index*; SD, *standard deviation*; *intraocular pressure*; CH, *corneal hysteresis*

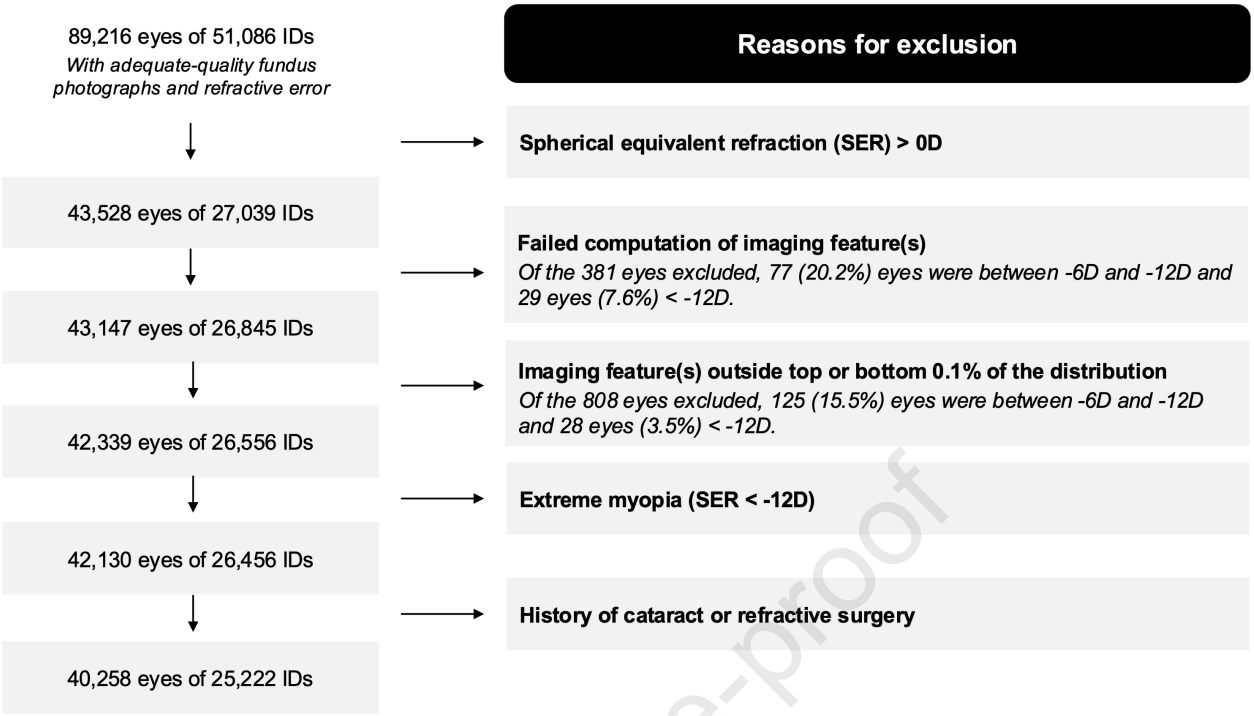

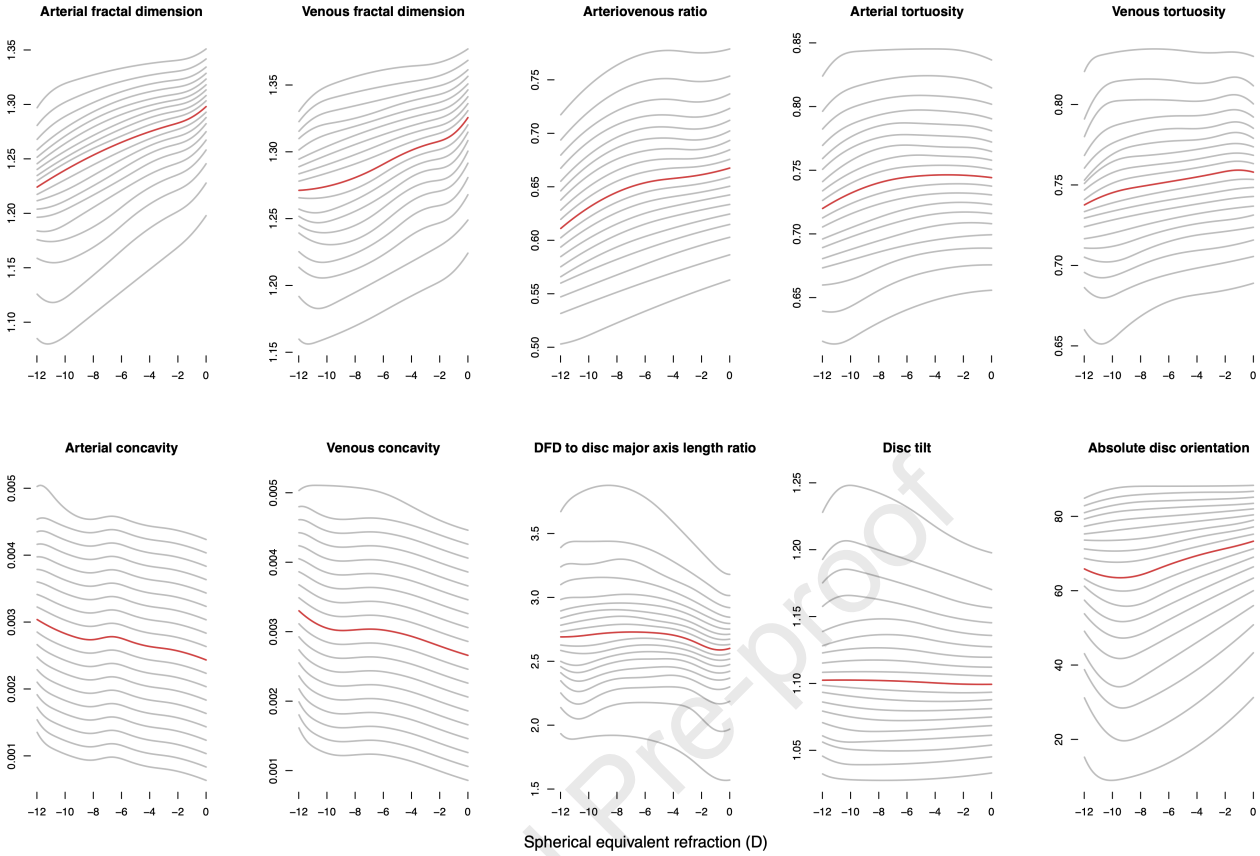

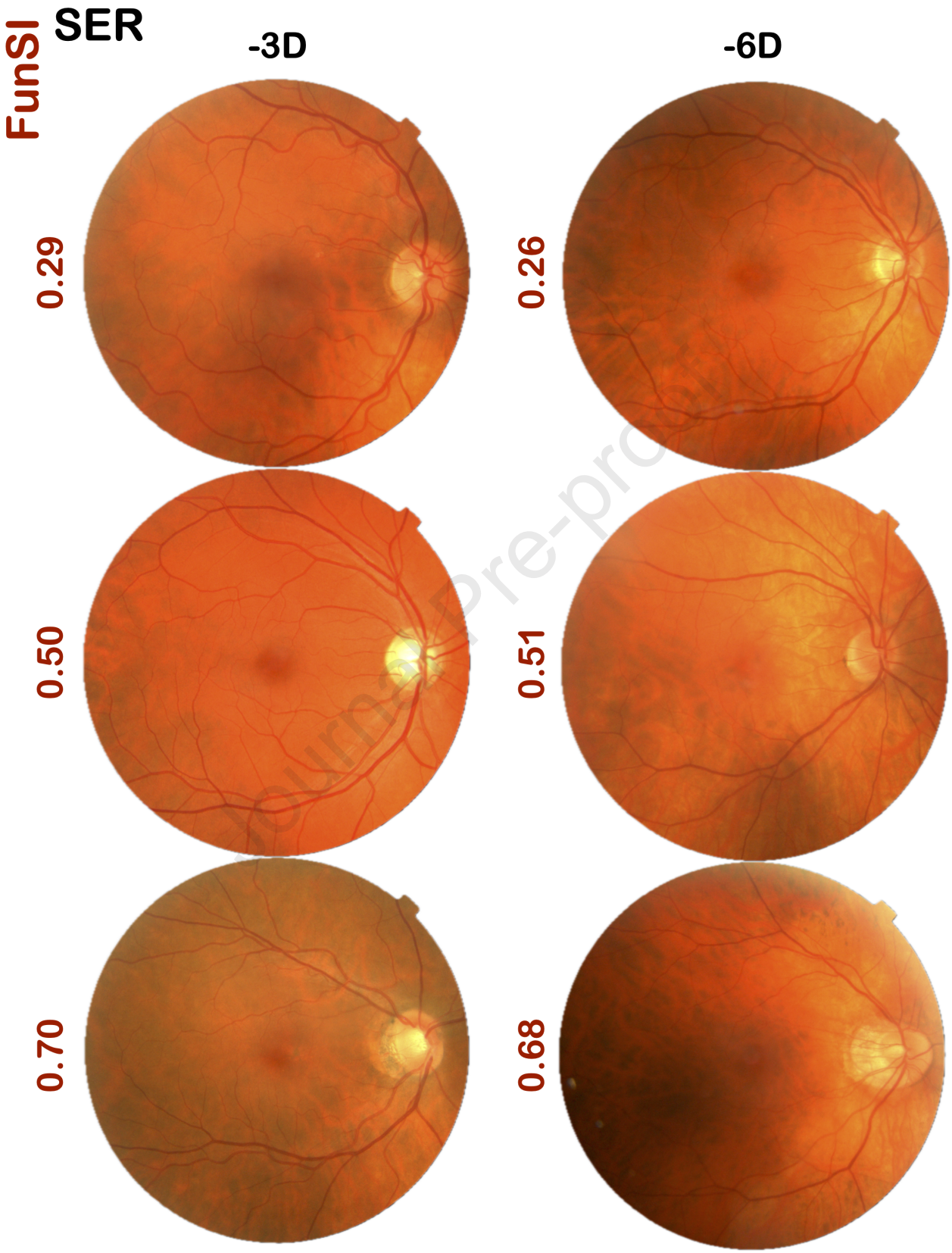

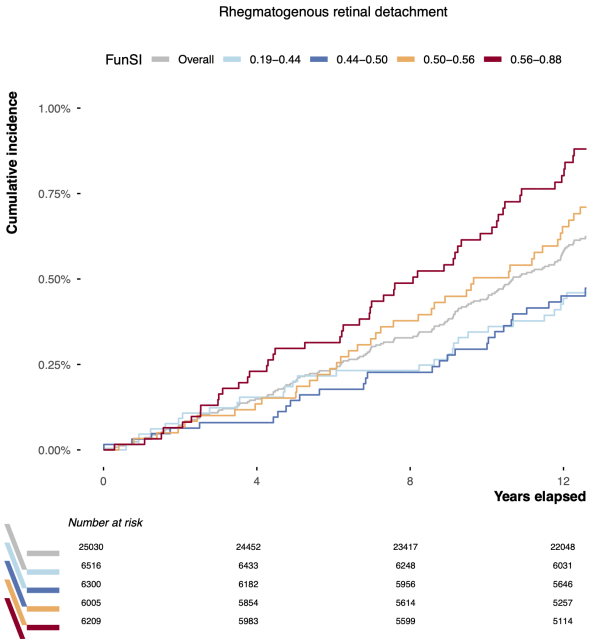

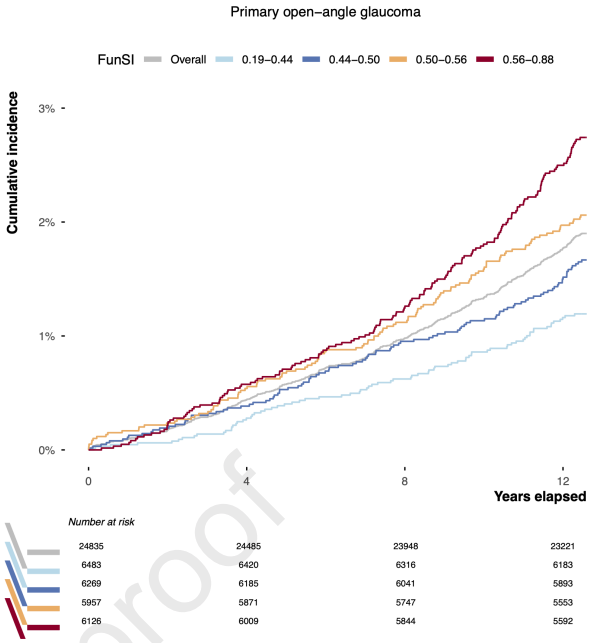

A higher baseline Fundus Stretch Index, indicating a more stretched fundus, was associated with an increased risk of retinal detachment and glaucoma over 12 years, even after adjusting for established risk factors including myopia severity.